Title : will be set by the publisher
Editors : will be set by the publisher
EAS Publications Series, Vol. ?, 2002

ON STELLAR DYNAMO PROCESSES AND DIFFERENTIAL ROTATION

Allan Sacha BRUN[1]

Abstract. Many stars exhibit strong magnetic fields, some of which are thought to be of primordial origin and others a sign of magnetic dynamo processes. We briefly review the results of observational studies of solar-type stars seeking to evaluate the linkage between rotation rate and possible magnetic cycles of activity. Clearly turbulent convection and rotation within spherical shell geometries provide ingredients essential for dynamo action. However, intensive efforts over several decades in solar research have demonstrated that it is no easy matter to achieve cyclic magnetic activity that is in accord with observations. Helioseismology has revealed that an essential element for the global solar dynamo is the presence of a tachocline of shear at the base of the solar convection zone, leading to the likely operation of an interface dynamo. We review the crucial elements for achieving a cyclic magnetic activity. We then discuss some of our current 3–D MHD simulations of solar turbulent convection in spherical shells that yield differential rotation profiles which make good contact with some of the helioseismic findings. We show that such turbulent motions can amplify and sustain magnetic field in the bulk of the convective zone whose strength are sufficient to feed back both upon the convection and its global circulations.

1 Introduction

During the last three decades considerable evidence for stellar magnetic activity has been gathered (Wilson 1978, Noyes et al. 1984, Baliunas et al. 1995). These observations based on CaII emissions, revealed that some stars exhibit irregular magnetic activity while others have solar-like activity cycles. What could be the source of such magnetic fields? Are the different types of activity (cyclic vs. irregular) indications of differences in the generation and amplification of magnetic field? Based on the ohmic diffusion time $\tau_{ohm} \sim R^2/\eta$ (where R is the stellar radius

[1] JILA, University of Colorado, Boulder, CO 80309-0440, USA.

DOI: (will be inserted later)

and η is the magnetic diffusivity, leading to $\tau_{ohm} \sim 10^{10}$ years for the Sun), many of those stars could have retained a fossil magnetic field over their main sequence lifetime without running a dynamo (Weiss 1994). However, it is tempting to search for a link between stellar global properties such as mass, rotation or convection and stellar magnetic activity. It is indeed important to notice that convection is always present in stars and that most of them rotate. Stars less massive than ~ 1.3 solar mass $M_\odot$ display convective envelope whereas the more massive ones possess a convective core. The latter appear due to an increasing contribution to the star's energy generation of the CNO nuclear cycles. Further, the range of rotation rates varies significantly from very slow rotators ($P > 150$ days) to near breakup velocities. One general trend is that older stars rotate slower. Another is that the presence of magnetic fields increases the probability for a star to be a slow rotator. More precisely Durney & Latour (1978) have shown that stellar magnetic activity for main sequence stars can reasonably been explained by evaluating the Rossby number R_o. In their model, strong magnetic activity is seen in stars for which $R_o << 1$ (i.e. their convective motions strongly feel rotation). In reality stars are more complex, and there is evidence that slowly rotating Ap stars exhibit stronger magnetic field than fast rotating A stars (Moss 2002). Here even though A stars have a convective core that is likely to generate a dynamo field, some quenching mechanism has to be invoked to reproduce the observations–unless the observed field in Ap star is of fossil origin and the dynamo generated field screened by the radiative envelope. I will here focus my attention on solar type stars (see Mestel 2001 for stars of other spectral type). In particular, I will examine the dynamical establishment of the solar differential rotation and meridional circulations and their nonlinear link with magnetic fields. I will present recent results from simulations of solar convection within full 3–D spherical shells, discussing the angular velocity Ω profiles that can be achieved in the bulk of such convection zones and the level of dynamo induced magnetism that can be sustained there.

2 Our Numerical Approach

The anelastic spherical harmonics (ASH) code solves the 3–D MHD anelastic equations of motion in a rotating spherical shell geometry using a pseudo-spectral/semi-implicit method (Miesch et al. 2000, Brun & Toomre 2002,2003). The model is a simplified description of the solar convection zone: solar values are taken for the heat flux, rotation rate, mass and radius, and a perfect gas is assumed since the upper boundary of the shell lies below the H and He ionization zone. The computational domain extends from 0.72 $R_\odot$ to 0.97 $R_\odot$, thereby concentrating on the bulk of the unstable zone and here not dealing with penetration into the radiative interior. The effects of the steep entropy gradient close to the surface has been softened by introducing a subgrid scale (SGS) transport of heat to account for the unresolved motions, and enhanced eddy diffusivities are used in these large eddy simulations (LES). The typical density difference across the shell in radius is about 30.

3 Solar Convection and Rotation

3.1 Convective Patterns

Figure 1 displays the evolution of enstrophy (vorticity^2) in the case called E (Brun & Toomre 2003) over 10 days in time near the top of the domain. The vantage point is in the uniformly rotating frame used in our simulations. The convection patterns are highly time dependent. Some of the pattern evolution is related to the advection by zonal flows associated with the differential rotation driven by the convection relative to this frame (i.e fast equator/slow poles). There is an asymmetry between the broad upflows showing a weaker vortical content and the narrow fast downflows at their periphery. This leads to a downward transport of kinetic energy. The strong correlations between warm upward motions and cool downward motions are essential in transporting the heat outward.

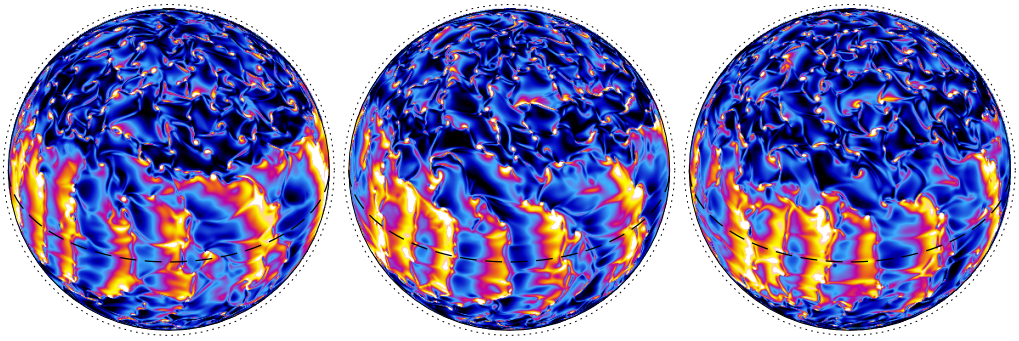

Fig. 1. Evolution in the convection over 10 days, showing the enstrophy (vorticity^2) in case E near the top (0.97 $R_\odot$) of the spherical domain. The time interval between each successive image is about 5 days. Strong vortical flows appear bright. The dotted circle is located at the solar radius $R_\odot$ and the equator is indicated by the dashed curve.

Vortical structures are found at the interstices of the downflow network, although strong fronts are seen in a band near the equator. The strongest of these vortex tubes or 'plumes' extend through the whole domain depth. These plumes represent coherent structures that are surrounded by more chaotic flows. They are counterclockwise in the northern hemisphere and clockwise in the southern one. They tend to align with the rotation axis and to be tilted away from the meridional planes, leading to Reynolds stresses that are crucial ingredients in redistributing the angular momentum within the shell (Brun & Toomre 2002).

3.2 Differential Rotation

The differential rotation profile in latitude and radius associated with the vigorous convection of case E is shown in Figure 2. For simplicity, we have converted the mean longitudinal velocity $\hat{v}_\phi$ into a sidereal angular velocity Ω, using $\Omega_o/2\pi = 414$ nHz (or 28 days) as the reference frame rotation rate. In the contour plot, the

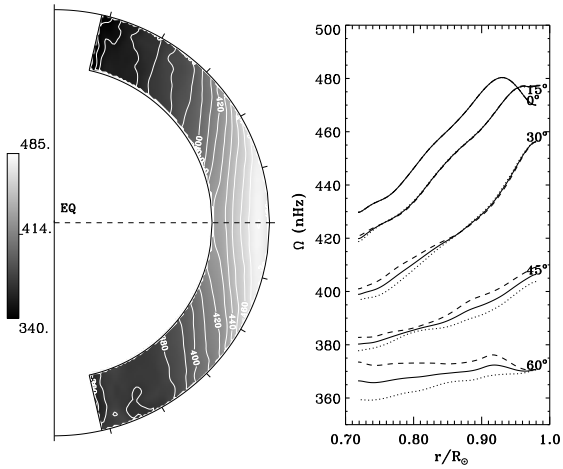

Fig. 2. Temporal and longitudinal averages in case E of the angular velocity profile formed over an interval of 85 days. This case exhibits a prograde equatorial rotation and a strong contrast $\Delta\Omega$ from equator to pole, as well as possessing a high latitudes region of particularly slow rotation. In the right panel a sense of the asymmetry present in the solution can be assessed in these radial cuts at indicated latitudes.

near polar regions have been omitted due to the difficulty of forming stable averages there, since the averaging domain is small but the temporal variations large. Case E exhibits a fast (prograde) equatorial region and slow (retrograde) high latitude regions. This is due to correlations in the velocity components leading to significant Reynolds stresses. These Reynolds stresses are intimately linked to the influence of Coriolis forces acting upon the convecting motions and to the presence of plumes tilted both away from the local radial direction and out of the meridional plane. Such correlations have been identified in local high resolution Cartesian domains as well (Brummell et al. 1998). These lead to an equatorward transport of angular momentum, resulting in the slowing down of the high latitude regions and speeding up of the equatorial zone. At low latitudes there is some alignment of Ω contours with the rotation axis. At mid latitudes, the angular velocity is nearly constant along radial lines, in good agreement with helioseismic deductions (Schou et al 1998). Further, case E exhibits a monotonic decrease of Ω with increasing latitude, a property that has been difficult to achieve in 3–D spherical convection calculations. Indeed, most other cases have their equator to pole contrast $\Delta\Omega$ confined to mid latitudes extending to about $\sim 42°$ (Brun & Toomre 2002). The differential rotation contrast between the equator and 60° in case E is 110 nHz (or 26% relative to the frame of reference), thus being very close to the 92 nHz (or 22%) variation observed in the Sun. A sense of the asymmetry present in case E can be assessed both in the contour plot and in the latitudinal cuts (right panel of Fig. 2), where we have plotted Ω in the north (dotted) and south (dashed) hemispheres, along with their mean. The convection itself exhibits some asymmetry between the two hemispheres (cf. Fig. 1), and so it is not surprising that the mean flows driven by the convection do the same. These asymmetries are expected to

diminish over longer temporal averages. Mean field models of the solar differential rotation (Kichatinov & Rüdiger 1995) have advocated that a thermal wind balance (involving pole to equator temperature contrasts) could be the cause of the non-cylindrical profile in Ω. This could come about through the baroclinic nature of the convecting motions yielding some latitudinal heat fluxes, resulting in the breakdown of the Taylor-Proudman theorem. Although it is indeed true that case E exhibits latitudinal variation of entropy and temperature fluctuations relative to the mean, these are not the most dominant players everywhere in the shell. A temperature contrast of few degree K seems compatible with a $\Delta\Omega/\Omega_o$ of $\sim 30\%$. However, we find that the Reynolds stresses are the main agents responsible for the equatorial acceleration achieved in our simulations, and thus the solar differential rotation is dynamical in origin.

3.3 Meridional Circulation

The meridional circulation associated with the vigorous convection in case E is maintained variously by Coriolis forces acting on the differential rotation, by buoyancy forces, by Reynolds stresses and by pressure gradients, and thus can be thought as departures from a simple geostrophic balance (Brun & Toomre 2002). The meridional circulation seen in case E exhibits multi-cell structure both in latitude and radius, and given the competing processes for its origin, it is not straightforward to predict. Typical amplitudes for the velocity are of order 25 m/s, comparable to local helioseismic deductions (Haber et al. 2002). The flow is directed poleward at low latitudes, with return flow deeper down. The temporal fluctuations in the meridional circulation are large and thus stable time averages are only attained by sampling many rotations. The kinetic energy in the differential rotation and in the convective motions are two orders of magnitude higher than that in the meridional circulation (Brun & Toomre 2002). As a result, small fluctuations in the convective motions and differential rotation can lead to major variations in the circulation. Some of the helioseismic inferences suggest the presence of single cell circulations, which are at odds with our multi-cell patterns. However these inferences vary from year to year, and there is recent evidence for double-cell structure in the circulations observable in the near-surface shear layer, but only in the northern hemisphere as the current solar cycle advances (Haber et al. 2002). From a careful analysis of the angular momentum transport in our shell we have deduced that the slow pole behavior seen in case E seems to come about from a relatively weak meridional circulation at high latitudes. This permits a more efficient extraction of angular momentum by the Reynolds stresses from the high latitudes toward the equator in yielding the interesting differential rotation profile that is achieved.

4 Incorporating some Magnetic Fields

We now turn to consider the influence of magnetic fields both upon the convection in our deep shell and upon the angular velocity profiles that can be maintained.

Early attempts to explain the 22-year solar cycle considered the possibility that the solar dynamo operated within the bulk of the convective envelope (Gilman 1983, Glatzmaier 1985), but such approaches failed because strong magnetic fields could not be stored efficiently within the unstable stratification of the convection zone. The dynamo periods were too short (of the order of 1 year) and the poloidal fields were found to propagate poleward, at variance with observations. More recently, Parker (1993) has proposed an *interfacial* dynamo model seated in the stable tachocline. Magnetic field is still generated within the bulk of the convection zone (α-effect), but is pumped downward into the stable layer via overshooting turbulent plumes, to be stretched there into large-scale toroidal structures by the strong shear of the tachocline (ω-effect). When the amplification of the toroidal magnetic field is great enough, the structures (called magnetic flux tubes in mean field models) become magnetically buoyant and rise upward through the convective envelope. The strongest of those structures emerge in the photosphere as bipolar magnetic arcades, whereas the weaker ones are recycled within the convective zone. This leads to the crucial natural cycle of poloidal to toroidal exchange, i.e. $B_{pol} \rightarrow B_{tor} \rightarrow B_{pol}$. However, many aspects of these essential 'dynamo building blocks' remain to be demonstrated through nonlinear 3–D calculations. At present it is not feasible to simulate self consistently all the processes operating together, and thus one needs to concentrate on individual components (magnetic generation, pumping, shearing, buoyant rising). One important ingredient in the interfacial dynamo scenario is the ability of the convective motions to generate and sustain magnetic fields in the bulk of the zone (Cattaneo & Hughes 2001). We thus have evaluated some conditions in 3–D compressible convective shells for which such a dynamo threshold can be realized. We further wished to identify the maximum nonlinear amplification of the magnetic field that can be sustained by the convective motions without destroying the strong angular velocity contrasts previously attained.

4.1 Determining the Dynamo Threshold in Convective Shells

We have conducted three MHD simulations (named $M1$, $M2$ and $M3$) started from a solution not as turbulent as case E but exhibiting a similar angular velocity profile Ω. We then introduced a small seed dipolar magnetic field and let the simulations proceed. Figure 3 shows the magnetic energy evolution for three values of the magnetic diffusivity η (i.e. 2, 1.6 & 1 $\times 10^{12}$ cm^2/s). We note that over more than 3000 days (corresponding to several ohmic decay times) the two lowest diffusive cases $M2$ and $M3$ exhibit a sustained magnetic energy (ME), the levels of which depend on η. The other case $M1$ is clearly decaying, since the rate of generation of magnetic fields could not compensate for the rate of destruction by ohmic diffusion. The dynamo threshold seems to be around a magnetic Reynolds number $R_{\rm em} = v_{\rm rms} D/\eta$ of $\sim$ 300 or $\eta \sim 1.6 \times 10^{12}$. This is about 25% higher than in a progenitor incompressible simulation (Gilman 1983).

Further, we find that the kinetic energy (KE) in model $M3$ has been reduced by about 40% compared to its initial value. In this case ME has grown to reach

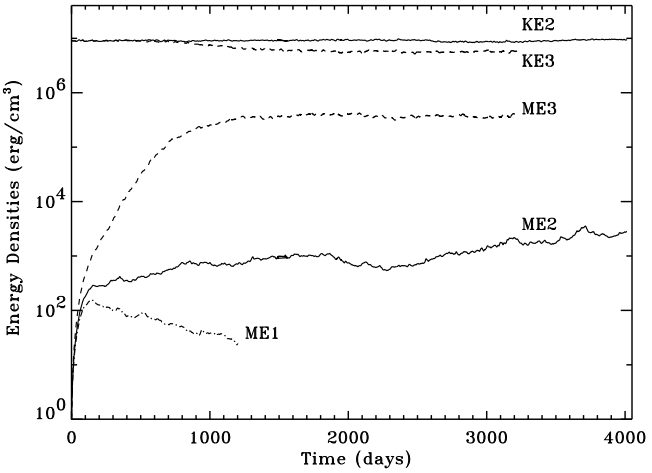

Fig. 3. Kinetic energy (KE) and magnetic energy (ME) for cases $M1$, $M2$ and $M3$, involving in turn a magnetic rms Reynolds number R_{em} of 250 (dashed dot line), 300 (solid) and 500 (dashed).

a value of 7% of KE. The increase in ME started to influence the total amount of KE contained in the shell when ME reached roughly 0.5% of KE in after about 600 days of evolution. The early exponential growth of ME in case $M3$ corresponds roughly to the first 600 days after which the nonlinear feedback of the Lorentz forces on the flow begins to be felt. For case $M2$, ME is still small enough (i.e. $\leq 0.1\%$) even after 4000 days for the convective motions to only be mildly affected by the Lorentz forces. This is most clearly seen in comparing the kinetic energy time trace for cases $M2$ and $M3$. The magnetic energy stored in the toroidal field within the bulk of the convective zone is roughly an order of magnitude greater than that of the poloidal field.

Figure 4 displays a 3–D rendering of the radial velocity field and of the radial and longitudinal magnetic fields achieved in our convective shells. The radial component of the magnetic field is found to mainly concentrate in the downflow lanes, having been swept away from the center of the convective cells by the broad upflows. Both polarities coexist at the downflow network interstices. The radial component B_r possesses finer and more intricate structures than either V_r or B_ϕ, exhibiting many swirls. Substantial magnetic helicity is present, involving complex winding up of the toroidal magnetic fields along their length, with both polarities interchanging their positions. The toroidal magnetic fields also possess the greater spatial scales, having been stretched by the gradients in angular velocity especially in the equatorial region. Some features could resemble magnetic flux tubes, although they are short lived and less concentrated.

4.2 Effect of the Lorentz Force

With fairly strong magnetic fields sustained within the bulk of the convection zone in case $M3$, it is to be expected that the differential rotation Ω will respond to

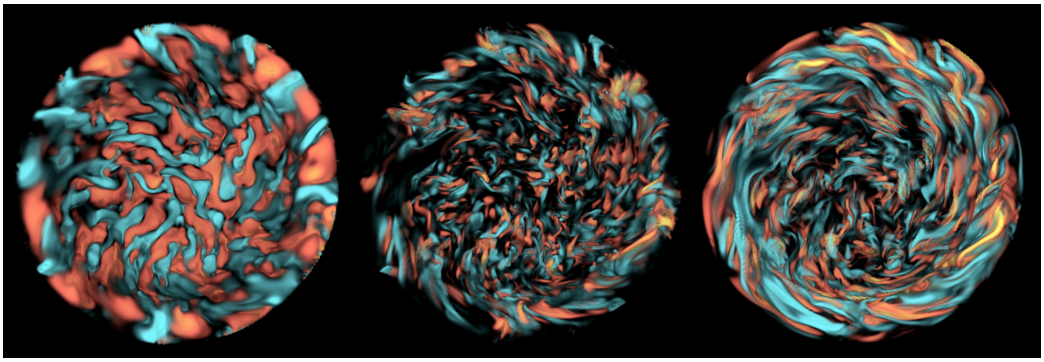

Fig. 4. 3-D rendering snapshots of the radial component of the velocity (left) and of the radial and longitudinal components of the magnetic field (middle and right) in case $M3$. Shown is the southern hemisphere seen from within the shell with the equatorial plane facing the reader. Brighter tones represent downflow and positive polarity. The velocity and magnetic field peak amplitudes are about 100 m/s and a few thousand gauss respectively.

the feedback from the Lorentz forces. Figure 5 shows the time averaged angular velocity achieved in case $M3$. The main effect of the Lorentz forces is to extract energy from the kinetic energy stored in the differential rotation. The reduction of KE contained in the angular velocity is of the same order as the decrease seen in the total KE, i.e. 40%. As a consequence, the angular velocity contrast $\Delta\Omega$ from 60° to the equator drops by $\sim 30\%$ in case $M3$, going from 140 nHz (or 34% compared to the reference frame Ω_o) in the hydrodynamic case to 100 nHz here (or 24%). Nevertheless, the angular velocity in case $M3$ remains in reasonable agreement with the solar profile. The reduction of the latitudinal contrast of Ω can be attributed to the poleward transport of angular momentum by the Maxwell stresses (the mean magnetic fields having a negligible contribution). Now the Reynolds stresses again need to balance the angular momentum transport by the meridional circulation, the viscous diffusion and the Maxwell stresses. This leads to a less efficient speeding up of the equatorial regions. Since ME is only 7% of KE in case $M3$, the Maxwell stresses are not yet the main players in redistributing the angular momentum. We have found that a value of ME above about 20% of KE leads to a significant magnetic braking effect on the differential rotation. Had the simulation been restarted with a stronger initial magnetic field B_0, $\Delta\Omega$ could drop by 90% in less than a few hundreds days, thus being at variance with helioseismic findings. Thus the feed back from the Lorentz forces can give an upper limit on the maximum sustainable magnetic field for a given rotation profile. In case $M3$ it seems that the limit is a few thousand gauss but we have to be cautious since this computation does not allow for expulsion of magnetic helicity or pumping of magnetic field into the radiative zone.

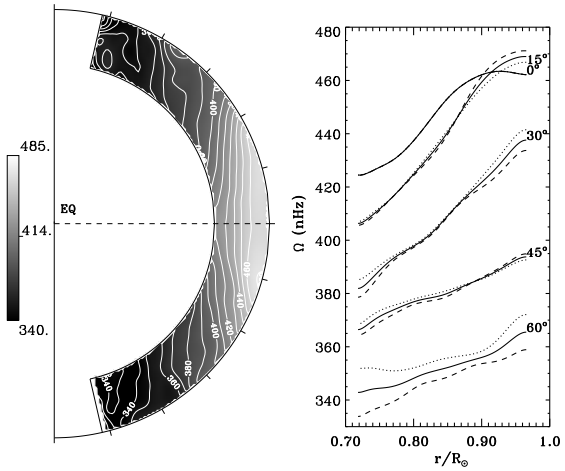

Fig. 5. Temporal and longitudinal averages of the angular velocity profiles achieved in case $M3$ over an interval of 80 days. This case exhibits a prograde equatorial rotation and a strong contrast $\Delta\Omega$ from equator to pole, as well as possessing high latitude regions of particularly slow rotation.

4.3 Magnetic Activity and Possible Cycles

I now wish to discuss possible differences between active stars and ones with solar-type cycles of magnetic activity. The interfacial dynamo invoked in this work to explain the solar cycle require a strong rotational shear located in the stable tachocline. Without such shear, the star is more likely to undergo local magnetic dynamo action directly associated with helical MHD turbulent convective flows (i.e the α-effect). Yet, any convection zone under the influence of rotation is likely to have a more or less pronounced differential rotation (cf. Brun, Browning & Toomre 2003 for core convection and dynamo processes in A-type stars). Thus some ω-effect can also be expected within a convection zone, except that the strongest magnetic fields present in the unstable convective zone will certainly be smaller than the ones amplified in the stable tachocline (again because of buoyancy considerations). Thus, it is unlikely that purely convective stars such as M dwarfs or pre-main sequence stars will exhibit cycles, but instead may display irregular activity (the strength of which will likely depends on the rotation rate or Rossby number R_o).

5 Conclusions

Our simulations of convection in 3-D spherical shells are describing how turbulent convection under the influence of rotation can achieve a well organized differential rotation. Transport of angular momentum by tilted turbulent plumes generate Reynolds stresses leading to an equatorial acceleration, such as seen in the Sun. When we introduce a seed magnetic field and let the simulation evolve until equilibration we find solutions where it is possible to sustain both a magnetic field and a solar-like differential rotation. The amount of magnetism that can be sus-

tained in a convective shells for a given rotation profile gives us some clues on how solar magnetism is working. Strong energetic event like CME's and the pumping of magnetic energy in the stable radiative zone certainly plays a significant role in regulating the intricated and coupled interplay of convection, rotation and magnetism. From a more general stellar point of view, it is clear that convection under the influence of rotation and magnetism will lead to significant activity but not necessarily to cycles. For the latter, a stable shear region such as the solar tachocline seems to be a crucial element in order to close the loop of magnetic field generation and organization.

I thank Mark Miesch, Annick Pouquet, Juri Toomre and Jean-Paul Zahn for useful discussions and collaborations and Jean Arnaud for its invitation to the workshop. This work was partly supported by NASA through SEC Theory Program grant NAG5-8133 and by NSF through grant ATM-9731676. The simulations with ASH were carried out with NSF PACI support of the San Diego Supercomputer Center (SDSC). Much of the analysis of the extensive data sets has been done in the Laboratory for Computational Dynamics (LCD) within JILA.

References

Baliunas, S.L. et al. 1995, ApJ, 438, 269

Brummell, N.H., Hurlburt, N.E., & Toomre, J. 1998, ApJ, 493, 955

Brun, A.S., & Toomre, J. 2002, ApJ, 570, 865

Brun, A.S., & Toomre, J. 2003, "3-D Stellar Evolution", ASP Conf. Ser. in press

Brun, A.S., Browning, M. & Toomre, J. 2003, "IAU215 on Stellar Rotation", ASP Conf. Ser. in press

Cattaneo, F., & Hughes, D.W. 2001, Astron. & Geophys., 42 (3), 18

Durney, B.R., & Latour, J. 1978, Geophys. Astrophys. Fluid dynamics, 9, 241

Gilman, P.A. 1983, ApJS, 53, 243

Glatzmaier, G.A. 1985, Geophys. Astrophys. Fluid Dynam., 31, 137

Haber, D.A., Hindman, B.W., Toomre, J., Bogart, R.S., Larsen, R.M., & Hill, F. 2002, ApJ, 570, 855

Kichatinov, L.L., & Rüdiger, G. 1995, A&A, 299, 446

Mestel, L. 2001, "Magnetic Fields Across the HR Diagram", G. Mathys, S.K. Solanki & D.T. Wickramasinghe (eds), ASP Conf. Ser., 248, 3

Miesch, M.S., Elliott, J.R., Toomre, J., Clune, T.L., Glatzmaier, G.A., & Gilman, P.A., 2000, ApJ, 532, 593

Moss, D. 2001, "Magnetic Fields Across the HR Diagram", G. Mathys, S.K. Solanki & D.T. Wickramasinghe (eds), ASP Conf. Ser., 248, 305

Noyes, R.W., Weiss, N.O. & Vaughan, A.H. 1984b, ApJ, 287, 769

Parker, E.N. 1993, ApJ, 408, 707

Schou, J. et al. 1998, ApJ, 505, 390

Weiss, N.O. 1994, "Lectures on Solar and Planetary Dynamos", eds M.R.E Proctor & A.D. Gilbert, Cambridge University Press, 59

Wilson, O.C. 1978, ApJ, 226, 379